SUPPLEMENTAL MATERIALS

S100A9-RAGE axis accelerates formation of macrophage-mediated extracellular vesicle microcalcification in diabetes

Ryo Kawakami, MD, PhD[1]; Shunsuke Katsuki, MD, PhD[1]; Richard Travers, MD[1]; Dayanna Carolina Romero, BS[1]; Dakota Becker-Greene, BS, BA[1]; Livia Silva Araujo Passos, PhD[1]; Hideyuki Higashi, MS[2], Mark C. Blaser, PhD[2], Galina K. Sukhova, PhD[1]; Josef Buttigieg, PhD[3]; David Kopriva, MD[4]; Ann Marie Schmidt, MD[5]; Daniel G. Anderson, PhD[6]; Sasha A. Singh, PhD[2]; Luis Cardoso, PhD[7]; Sheldon Weinbaum, PhD[7]; Peter Libby, MD[1]; Masanori Aikawa, MD, PhD[1,2]; Kevin Croce, MD, PhD[1]; Elena Aikawa, MD, PhD[1,2,8]

[1]The Center for Excellence in Vascular Biology, Brigham and Women's Hospital, Harvard Medical School, Boston, MA; [2]Center for Interdisciplinary Cardiovascular Sciences, Brigham and Women's Hospital, Harvard Medical School, Boston, MA; [3]Department of Biology, University of Regina, Regina, Saskatchewan, Canada; [4]Regina Qu'Appelle Health Region and University of Saskatchewan, Regina, Saskatchewan, Canada; [5]Diabetes Research Program, Division of Endocrinology, Diabetes and Metabolism, Department of Medicine, New York University, New York, NY; [6]Institutes for Medical Engineering and Science, Massachusetts Institute of Technology, Cambridge, MA; [7]Department of Biomedical Engineering, The City College of New York, New York, NY; [8]Department of Human Pathology, Sechenov First Moscow State Medical University, Moscow, Russia.

Online supplemental materials and methods

The data, analytic methods, and study materials will be made available to other researchers upon request for purposes of reproducing the results or replicating the procedure. Requests can be made to the corresponding author who manages the information.

Cell cultures

Buffy coats were purchased from Research Blood Components, LLC (Boston, MA) and derived from de-identified healthy donors. The company recruits healthy donors under a New England Institutional Review Board-approved protocol for the Collection of Whole Blood for Research Purposes (NEIRB#04-144). We had no access to the information about donors. Human PBMC, isolated by density gradient centrifugation, were cultured in RPMI-1640 (Thermo Fisher Scientific, Waltham, MA) containing 5% non-depleted human serum and 1% penicillin/streptomycin for 10 days to differentiate macrophages. In stimulation assays, confluent macrophages were rinsed extensively with PBS, starved for 24 hours in 0.1% human serum media with 5mM D-glucose (normal glucose condition) or 25mM D-glucose (high glucose condition) (Thermo Fisher Scientific, Waltham, MA), and treated with recombinant human S100A9 protein (R&D Systems Inc., Minneapolis, MN). All supplement human serum was depleted of EVs by ultracentrifugation for 18 hours at 120,000×g unless it is specifically mentioned as non-depleted, as in previous reports [1]. In inhibition assays, macrophages were starved for 24 hours and pretreated with RAGE antagonist, FPS-ZM1 (10 μg/mL, Millipore Sigma, Burlington, MA) or DMSO (Sigma-Aldrich, St. Louis, MO) for 4 hours, Nrf2 activator, VSC2 (10 μM, Millipore Sigma) or DMSO (Sigma-Aldrich), for 1 hour as in previous reports [2,3] before stimulation with recombinant human S100A9 protein.

THP-1 cells (American Type Culture Collection, ATCC, Manassas, VA) were maintained in RPMI-1640 (Thermo Fisher Scientific) containing 10% fetal bovine serum (FBS). In stimulation assays, confluent macrophages were rinsed extensively with PBS, starved for 24 hours in 0.1% serum media, and treated with recombinant human S100A9 protein (R&D Systems Inc.). In inhibition assays, macrophages were starved for 24 hours and pretreated with VSC2 (10 μM, Millipore Sigma) or DMSO (Sigma-Aldrich) for 1 hour before stimulation with recombinant human S100A9 protein. All experiments of THP-1 cells were performed

between 5 to 10 passages.

Limulus amebocyte lysate (LAL) endotoxin assay

To measure the endotoxin level in the recombinant human S100A9 protein, the chromogenic LAL endotoxin assay was performed (GenScript, Piscataway, NJ). The pH value of recombinant human S100A9 protein was adjusted to 7.0 with endotoxin-free 0.1N sodium hydroxide, according to the manufacturer's instructions. The minimum endotoxin detection limit is 0.005 EU/mL.

Human tissue samples

Specimens of discarded human carotid plaques (n=25) were obtained at endarterectomy by protocols approved by the Human Investigation Review Committee at Brigham and Women's Hospital. Samples were embedded in optimal cutting temperature compound (OCT) and stored at -80°C until use. Cryosections of 6-μm thickness were stained for AGE (bs-1158R, Bioss Antibodies, Woburn, MA), RAGE (GTX23611, GeneTex, Inc., Irvine, CA), S100A9 (14226-1-AP, Proteintech Group, Inc., Rosemont, IL), ALP (ab108337, Abcam, Cambridge, MA), macrophages (CD68; Dako, Carpinteria, CA, USA) and smooth muscle cells (SMCs; α-smooth muscle actin [α-SMA; ENZ-C34931, Enzo Biochem, Inc., Farmingdale, NY]).

Animal procedures

Wild-type (WT) mice and apolipoprotein E-deficient ($Apoe^{-/-}$) mice with C57BL/6J background were purchased from the Jackson Laboratory (Bar Harbor, ME, USA). $S100a9^{-/-}$ ($MRP\text{-}14^{-/-}$) mice were crossbred with $Apoe^{-/-}$ mice in a C57BL/6J background to generate compound mutant double-deficient mice ($S100a9^{-/-}Apoe^{-/-}$) [4]. Single mutant $Apoe^{-/-}$ mice were used as controls. All mice had a congenic C57BL/6J background and were maintained in animal facilities at Harvard Medical School. Animal care and procedures were approved by the Institutional Animal Care and Use Committees, and all animal experiments were approved by the BWH Animal Welfare Assurance (protocol 2016N000178). The data from both male and female mice were pooled for this study because of statistical power loss due to the limited sample size in female mice.

9-week-old male WT, Apoe$^{-/-}$, and S100a9$^{-/-}$Apoe$^{-/-}$ mice were fed a high-fat high-cholesterol diet (HCD) (1.25% cholesterol, D12108C, Research Diets, Inc., New Brunswick, NJ, USA) for 10 weeks. At 19 weeks of age, they were divided into two groups: 1- Nondiabetes; 2-Diabetes. Diabetes group mice were intraperitoneally injected with 42 mg/kg streptozotocin (STZ; streptozocin, S0130, Sigma-Aldrich) for 5 days, as described previously [5]. Blood glucose was measured in the beginning and every week after STZ injection with the OneTouch glucometer (Contour, Bayer HealthCare, Mishawaka, IN). The body weight was measured in the beginning and every week after STZ injection. Mice with blood glucose levels exceeding 300 mg/dL were considered to have diabetes. After this first procedure, mice continued on HCD for another 8 weeks.

In another set of experiments, 9-week-old male (n=38) and female (n=22) Apoe$^{-/-}$ mice were fed a HCD for 10 weeks. At 19 weeks of age, diabetes was induced by STZ injection, as previously described. S100A9 siRNA and control siRNA targeting luciferase were encapsulated in macrophage-targeted C12-200 lipid nanoparticles (LNP), as previously described [6,7]. Macrophage-targeted lipid nanoparticles were prepared and mixed with siRNA to prepare siRNA encapsulated LNP [6,7]. Diabetic and nondiabetic mice with a HCD were treated with siS100a9 or siControl encapsulated LNP, 0.5 mg/kg were injected via tail vein to mice twice a week for 9 weeks.

At the end of the experiments, all mice were imaged with intra-vital microscopy (IVM) and fluorescent reflection imaging (FRI). For histology, samples (aortic roots, arches, and pancreas) were embedded in OCT compound (VWR) and stored at -80°C until use. Arteries for RNA isolation were snap frozen.

In vivo kinetics study of lipid nanoparticles (LNP)

Kinetics and cell specificity were analyzed with S100A9 siRNA encapsulated LNP. In the kinetics study, 0.5 mg/kg particles were injected via tail vein and peritoneal and splenic macrophages were collected by magnetic beads sorting (EasySep system, StemCell Technologies, Vancouver, Canada). In the specificity study, Apoe$^{-/-}$ mice were fed high-fat diet for 19 weeks. S100a9 siRNA or Control siRNA encapsulated LNP was administered 3 and 7 days before harvesting the aortic roots and arches.

Immunofluorescence - in situ hybridization dual staining

For detection of RNA transcripts, a commercially available kit (RNAscope® 2.5 HD Reagent Kit - RED, Advanced Cell Diagnostics, Hayward, CA) was used according to the manufacturer's instructions. OCT-embedded fresh frozen tissue (aorta) blocks were sectioned at 14 µm onto SuperFrost Plus slides (Thermo Scientific). Slides were fixed in the pre-chilled 4% paraformaldehyde (PFA) for 15 min at 4°C prior to use. After dehydration, the tissues were air dried and treated with RNAscope® Hydrogen Peroxide for 10 min. RNAscope Protease was then applied for 30 min at room temperature. Target probe (Mm-S100a9; 481401; Advanced Cell Diagnostics) was hybridized together for 2 h at 40°C, followed by a series of signal amplification and washing steps. All hybridizations at 40°C were performed in a HybEZ Hybridization System. Hybridization signals were detected by sequential chromogenic reactions using red chromogens. RNA staining signal was identified as red dots. Following the RNAscope assay, immunofluorescence for Mac3 was stained with anti-Mac3 (1:200; rat IgG1k, 553322, BD Biosciences, Franklin Lakes, NJ), and subsequently stained with Alexa Fluor anti-rat 488-labeled secondary antibody (Thermo Fisher Scientific). Nuclear staining with DAPI (Thermo Fisher Scientific) was performed. Each sample was quality controlled for RNA integrity with a probe specific to the housekeeping gene, cyclophilin B (PPIB). Negative control background staining was evaluated using a probe specific to the bacterial dapB gene.

Immunohistochemistry/ Immunofluorescence

Immunohistochemistry was performed on fresh frozen sections of mouse aortic arches and human carotid endarterectomy specimens, as previously described [8]. Briefly, tissue samples were frozen in OCT compound and 6-µm serial sections were cut and stained with hematoxylin and eosin (H&E) staining for general morphology. Antibodies included AGE (human; 1:100; Bioss Antibodies), RAGE (human; 1:50; GeneTex, mouse; 1:40; GeneTex), S100A9 (human; 1:250; Proteintech Group, Inc., mouse; 1:50), TER-119 (mouse; 10 µg/mL; MAB1125, R&D Systems Inc.), ALP (human; 1:100; Abcam), Mac3 (1:800; 553322, BD Biosciences), CD68 (1:500; Dako, CA), and αSMA (human; 1:25; Enzo Biochem, Inc.).

Immunohistochemistry used the avidin-biotin peroxidase method. The reaction was visualized with 3-amino-9-athyl-carbazol substrate (AEC; DAKO, CA). Adjacent sections treated with PBS in place of a primary antibody were used as negative controls. Immunofluorescence for RAGE and ALP with S100A9 was stained with anti-RAGE (rabbit IgG, Gene Tex), anti-ALP (rabbit IgG, Abcam) and anti-S100A9 (mouse IgG, 11145-MM01, Sino biological, Wayne, PA), and subsequently stained with Alexa Fluor anti-rabbit 568-labeled secondary antibody and Alexa Fluor anti-mouse 488-labeled secondary antibody (Thermo Fisher Scientific). Alkaline phosphatase activity (early marker of osteoblastic differentiation) was detected on unfixed cryosections according to manufacturer instructions (alkaline phosphatase substrate kit, Vector Laboratories, Burlingame, CA). Von Kossa silver stain was used to visualize inorganic phosphate calcium salts. Briefly, for von Kossa staining, section was incubated with 5% silver nitrate (American Master Tech Scientific, Lodi, CA) for 60 min under UV light, then washed with sodium thiosulfate. Nuclei were stained with nuclear fast red (American Master Tech Scientific). Images were captured with a microscope (Eclipse 50i, Nikon Instruments Inc., Melville, NY). For immunohistochemical quantification, the plaque area was the total selected area. The positive area of immunostaining was measured using the 'object detection by thresholding' tool from NIS-Elements AR 3.1 Software. The parts of the image histogram corresponding to the positive areas were manually selected and a template was created using two to three samples. The template was used to quantify all samples. The positive area fraction was calculated by the software. A region of interest was used to exclude areas that lacked tissue when necessary. A different template was created for each marker. Fluorescence visualized S100A9, RAGE, and ALP labeled with Alexa Fluor® 488/594. Images were captured and processed with the confocal laser microscopy (FLUOVIEW FV1000, OLYMPUS).

In vivo and ex vivo molecular imaging of the aorta

Intravital microscopy (IVM) was performed to evaluate proteolytic and osteogenic activity in vivo, as previously reported [9]. We used near-infrared fluorescent (NIRF) nanoparticles — ProSense 750EX (Ex/Em=750/770 nm) and OsteoSense 680EX (Ex/Em=668/687 nm) (PerkinElmer, Inc., Boston, MA). These nanoparticles were administered via tail vein 24 hours

before imaging. After surgical exposure of the right carotid artery, fluorescent signals from these nanoparticles were captured by confocal laser microscopy (Olympus FV1000). Proteolytic and osteogenic activity in the aorta was also monitored ex vivo. The aorta was perfused with saline, dissected and imaged to map the macroscopic NIRF signals elaborated by ProSense 750EX and OsteoSense 680EX using fluorescent reflection imaging (FRI, Image Station 4000MM, Eastman Kodak Co., New Haven, CT). Mean intensity of carotid artery for IVM and SUM of the intensity related to total aorta (excluding heart and aortic root) area for FRI were quantified and evaluated.

Quantitative 3D analysis of calcification in mice

Quantitative analysis of calcification was performed on the aortic arch and vessel branches originating from the arch (i.e. brachiocephalic, right and left subclavian, and right and left common carotid arteries) in Apoe$^{-/-}$ mice with diabetes (Diabetes siControl) and diabetes + siS100a9 (Diabetes siS100a9). Presence and amount of calcification was assessed in 3D using a high-resolution micro computed tomography (HR-μCT) system (1172, SkyScan, Belgium) with 2.1-μm nominal resolution [10]. Images were acquired using a 10M pixel digital camera, 100 kVp and 100 μA energy settings, and 5 averaged frames per X-ray angular projection to increase the signal to noise ratio. The resolution, field of view, number of angular projections and exposure time per frame was kept constant for all scans. Due to their size, 3 vertically connected scans (oversized scan option in the acquisition software) were needed to image the whole sample at high resolution. A reconstruction algorithm (Feldkamp cone beam) was used to generate cross-sectional images using NRecon software (V1.6.1.2, SkyScan, Belgium). Images were compensated during the reconstruction process for thermal shifting of the X-ray source, misalignment of the rotation axis, ring artifacts and beam hardening. Water, air and hydroxyapatite standards (1mm diameter rods containing 250 and 750mg/cm3 hydroxyapatite) were used to calibrate grey color images to mineral density (CTAn, V.1.10.1, SkyScan, BE), allowing identification of atheroma, lipid, calcified and soft tissues within vessels [10]. HR-μCT images of cardiovascular tissues were correlated to segments of the calcified particles from the soft tissues using a global thresholding method. The volume, surface and centroid of each individual 3D object were calculated automatically using CTAn

analysis software. An equivalent spherical diameter D = (6V/π)1/3 was obtained based on the volume V of each particle. The total calcified volume was the added volume of all individual calcified objects within the aortic arch, brachiocephalic, subclavian, and common carotid vessels.

Immuno-electron microscopy on calcified arteries

Tissues were immersion fixed in 2.5% glutaraldehyde, 2% paraformaldehyde, in 0.1M Cacodylate buffer pH 7.4 (modified Karnovsky's fixative). The tissues were dehydrated and embedded in acrylic resin. Thin sections (80-nm thickness) were placed on carbon coated and glow discharged formvar coated nickel slot grids. Blocked grids were incubated in primary antibody at RT for 1 hour, followed by an appropriate gold-conjugated secondary antibody for 1 hour at RT. After fixing with 1% glutaraldehyde in TBS, sections were contrast stained with uranyl acetate. Grids were imaged on a JEOL 1400 TEM equipped with a side mount Gatan Orius SC1000 digital camera. Primary antibodies included mouse anti-human S100A9 (1:200; R&D Systems, Minneapolis, MN, USA). Secondary antibodies included goat anti-mouse 10-nm colloidal gold (1:25; Abcam, Cambridge, MA, USA).

Isolation of mouse primary macrophages from peritoneal and splenic cells

Peritoneal cells were collected after injection of PBS with 1% FBS into the mouse peritoneal cavity. Splenic cells were suspended with PBS including 1% FBS. F4/80 positive macrophages were isolated by magnetic sorting (EasySep system, StemCell Technologies, Cambridge, MA). PE-conjugated anti-F4/80 antibody (123110, Biolegend, San Diego, CA) was used as the primary antibody to specifically select macrophages.

siRNA transfection of cultured cells

In siRNA experiments, human primary macrophages were transfected with 20 nmol/L siRNA using SilenceMag (BOCA Scientific, Boca Raton, FL), according to the manufacturer's instruction. Macrophages were cultured in normal glucose (5mM) or high glucose (25mM) medium after 48 hours from transfection. siRNA against human S100A9 (L-011384) and non-target (D-001810) were all ON-TARGETplus SMARTpool, purchased from GE

Dharmacon (Lafayette, CO).

Reverse transcription, quantitative real-time PCR

Total RNA was extracted from cell isolates by illustra RNAspin Mini kit (GE Healthecare, Little Chalfont, UK). cDNA was synthesized by High Capacity cDNA Reverse Transcription Kit (Applied Biosystems, Waltham, MA). Quantitative real-time PCR was performed with a 7900HT Fast Real-Time PCR System (Applied Biosystems). Primer designs are listed on Supplementary Table 2. Data were calculated by ΔΔCT method and expressed in arbitrary units that were normalized by β-actin or GAPDH, and presented as fold increase relative to control (normal glucose). All experiments of PCR were performed in triplicate for technical replicate.

Western blot analysis

Total cellular protein was collected from cells at 4°C in RIPA buffer (Thermo Fisher Scientific) containing 1% halt protease inhibitor cocktail (Thermo Fisher Scientific) and phosphatase inhibitor cocktail (PhosSTOP, Roche). Protein concentration was measured using BCA assay (Thermo Scientific). Total protein was separated by 4-15% SDS-PAGE and transferred using the Trans-Blot Turbo Transfer System RTA Transfer Kits (Bio-RAD). The membrane was blocked for non-specific binding in blocking buffer (TBS-T [Tris-buffered saline with 0.05% Tween-20] containing 2% dry milk), and incubated with primary antibody. Antibodies for detection included RAGE (1:1000; GeneTex Inc.), S100A9 (1:1000; Abcam), RelA (NF-kappa-B p65 subunit) (1:1000; BETHYL Laboratory.INC, Montgomery, TX, USA), and Phospho-NF-κB p65 (Ser536) (1:1000; Cell Signaling Technology, Danvers, MA, USA). Following incubation with primary antibodies, and washing wells with TBS-T, membranes were incubated with corresponding horseradish peroxidase-conjugated secondary antibody. β-actin (1:5000; Cell Signaling Technology, Danvers, MA, USA) was used as a loading control to demonstrate equal sample loading.

Isolation of macrophage-derived EVs

Cell media were collected after approximately 24 hours and subjected to centrifugation at

1,000 g for 5 minutes to remove cell debris, followed by 16,500 g for 5 minutes to remove apoptotic bodies and any larger vesicles. EV fraction was harvested from the media by ultracentrifugation at 100,000 g for 40 minutes at 4°C (Optima Max Ultracentrifuge, Beckman Coulter, Inc., Indianapolis, IN, USA). Nanoparticle Tracking Analysis using a Nanosight LM10 measured EVs between 30–300 nm. For protein isolation, ALP activity, and proteomic study, EVs were washed with PBS followed by another ultracentrifugation at 100,000 g for 40 minutes at 4°C. EVs were either lysed in protein lysis buffer or ALP lysis buffer.

Alkaline phosphatase (ALP) activity

ALP activity was measured in EVs using the Alkaline Phosphatase Activity Colorimetric Assay Kit (BioVision). The results were normalized to the protein concentration.

Blood biochemical analysis

Blood was collected from the tail vein and heart, and spun in a refrigerated centrifuge, then serum was stored at -80°C. Serum levels of urea, creatinine, phosphate, and calcium were assessed by QuantiChrom assay kits (BioAssay Systems, Hayward, CA). Serum levels of aspartate transaminase (AST), alanine transaminase (ALT), total cholesterol, low-density (LDL)/very-low-density (VLDL) lipoproteins, and high-density lipoprotein (HDL) were also assessed by EnzyChrom assay kits (BioAssay Systems).

Proteomics sample preparation

Carotid plaque specimens were obtained from 8 patients undergoing carotid endarterectomy for stroke prevention at a single three-surgeon vascular surgery practice in Regina (Saskatchewan, Canada). The study was approved by the ethics boards of Brigham and Women's Hospital, the University of Saskatchewan, Regina Qu'Appelle Health Region, and the University of Regina through a harmonized review process (protocol# REB-13-115), and all patients gave written informed consent to participate.

Immediately after surgical removal, carotid plaques were separated into a sample from the most severely narrowed portion of the carotid artery, and the samples were snap-frozen in liquid nitrogen and stored in a -80°C freezer before being transported on dry ice to Brigham

and Women's Hospital.

Next, the samples were pulverized in liquid nitrogen and re-suspended in RIPA buffer (Thermo Fisher Scientific, USA) with 1%-protease inhibitor cocktail (Roche, Switzerland) for protein sampling. The protein samples were subsequently prepared for label-free proteomics. Protein extraction and proteolysis were performed with the methanol-chloroform method and trypsin (Gold Grade; Promega, Wisconsin) respectively, as previously published [11]. Fifteen micrograms of protein were used per sample. The tryptic peptides were desalted using Oasis Hlb 1cc (10 mg) columns (Waters, USA), and dried with a tabletop speed vacuum (Vacufuge plus, Eppendorf AG, Germany). After re-suspension in 40 µl of 5% liquid chromatography-mass spectrometry (LC-MS) grade acetonitrile (Thermo Fisher Scientific, USA) and 0.5% formic acid (Sigma- Aldrich, USA) in LC-MS grade water (Thermo Fisher Scientific, USA), the tryptic peptide samples were analyzed by liquid chromatography-mass spectrometry.

Liquid chromatography tandem mass spectrometry (LC-MS/MS) analysis

The Orbitrap Fusion Lumos mass spectrometer fronted with an Easy-Spray ion source, coupled to an Easy-nLC1000 HPLC pump (Thermo Scientific) was used to analyze the peptide samples. The analytical gradient was run at 300 nL/minute from 5 to 22% Solvent B (acetonitrile/0.1 % formic acid) for 110 minutes, 22 to 32% for 10 minutes, 32 to 90% for 10 minutes, followed by 10 minutes of 90% Solvent B. Solvent A was 0.1 % formic acid. The precursor scan was set to 240 K resolution with an orbitrap, and the top N precursor ions within 3 second cycle time (scan range of 375-1500 m/z) were subjected to higher energy collision induced dissociation (HCD, collision energy 30%, quadrupole isolation width 0.7 m/z, dynamic exclusion enabled, starting a first mass at 200 m/z, and rapid ion trap scan rate) for peptide sequencing (MS/MS).

LC-MS/MS data analysis

The MS/MS data were queried against the human UniProt database (downloaded in November 2018) using the SEQUEST HT search algorithm, via the Proteome Discoverer version 2.2 (PD2.2, Thermo Scientific). Mass tolerance was set to a 10-ppm window for

precursor and a 0.6 Da window for fragment. Methionine oxidation was set as a variable modification, and carbamidomethylation of cysteine residues was set as a fixed modification. The peptide false discovery rate (FDR) was calculated using Percolator provided by PD and peptides were filtered based on a 1% FDR. Peptides assigned to a given protein group, and not present in any other protein group, were considered as unique. Consequently, each protein group is represented by a single master protein (PD Grouping feature). Master proteins with two or more unique peptides were used for precursor intensity-based quantification. The protein abundances were normalized by total peptide amount mode and exported from PD2.2. The data were then analyzed using Qlucore (http://www.qlucore.com/) to perform a two-group comparison (non-diabetic versus diabetic) to identify proteins that were differentially abundant (increase/decrease by 2-fold) between the two groups ($p<0.05$). The data were then imported into Excel to make the volcano plot.

Statistics

Data are expressed as mean ± SEM for continuous variables. Majority of our *in vitro* data were normalized to normal glucose condition. Data were analyzed by unpaired *t*-test or one-way ANOVA with the Bonferroni post hoc test using GraphPad Prism 5.0 (GraphPad, San Diego, CA). Data with multiple interactions were analyzed by two-way ANOVA with the Bonferroni post hoc test. Data have been analyzed for normality and equal variance as a justification for using parametric or nonparametric analyses using Prism software. $p<0.05$ was considered statistically significant. The n values represent the number of patients, mice, or donors studied.

Supplemental References

1. Shelke GV, Lässer C, Gho YS, Lötvall J. Importance of exosome depletion protocols to eliminate functional and RNA-containing extracellular vesicles from fetal bovine serum. *J Extracell Vesicles*. 2014;3.
2. Chen Y, Huang XJ, Yu N, Xie Y, Zhang K, Wen F, Liu H, Di Q. HMGB1 Contributes to the Expression of P-Glycoprotein in Mouse Epileptic Brain through Toll-Like Receptor 4 and Receptor for Advanced Glycation End Products. *PLoS One*. 2015;10:e0140918
3. Lee JA, Kim JH, Woo SY, Son HJ, Han SH, Jang BK, Choi JW, Kim DJ, Park KD, Hwang O. A novel compound VSC2 has anti-inflammatory and antioxidant properties in microglia and in Parkinson's disease animal model. *Br J Pharmacol*. 2015;172:1087-1100.
4. Croce K, Gao H, Wang Y, Mooroka T, Sakuma M, Shi C, Sukhova GK, Packard RR, Hogg N, Libby P, Simon DI. Myeloid-related protein-8/14 is critical for the biological response to vascular injury. *Circulation*. 2009;120:427-436.
5. Islam MS, Loots du T. Experimental rodent models of type 2 diabetes: a review. *Methods Find Exp Clin Pharmacol*. 2009;31:249-261.
6. Leuschner F, Dutta P, Gorbatov R, Novobrantseva TI, Donahoe JS, Courties G, Lee KM, Kim JI, Markmann JF, Marinelli B, Panizzi P, Lee WW, Iwamoto Y, Milstein S, Epstein-Barash H, Cantley W, Wong J, Cortez-Retamozo V, Newton A, Love K, Libby P, Pittet MJ, Swirski FK, Koteliansky V, Langer R, Weissleder R, Anderson DG, Nahrendorf M. Therapeutic siRNA silencing in inflammatory monocytes in mice. *Nat Biotechnol*. 2011;29:1005-1010.
7. Koga JI, Nakano T, Dahlman JE, Figueiredo JL, Zhang H, Decano J, Khan OF, Niida T, Iwata H, Aster JC, Yagita H, Anderson DG, Ozaki CK, Aikawa M. Macrophage Notch Ligand Delta-Like 4 Promotes Vein Graft Lesion Development: Implications for the Treatment of Vein Graft Failure. *Arterioscler Thromb Vasc Biol*. 2015;35:2343-2353.
8. Aikawa E, Aikawa M, Libby P, Figueiredo JL, Rusanescu G, Iwamoto Y, Fukuda D, Kohler RH, Shi GP, Jaffer FA, Weissleder R. Arterial and aortic valve calcification abolished by elastolytic cathepsin S deficiency in chronic renal disease. *Circulation*. 2009;119:1785-1794.
9. Aikawa E, Nahrendorf M, Sosnovik D, Lok VM, Jaffer FA, Aikawa M, Weissleder R. Multimodality molecular imaging identifies proteolytic and osteogenic activities in early aortic valve disease. *Circulation*. 2007;115:377-386.
10. Maldonado N, Kelly-Arnold A, Laudier D, Weinbaum S, L Cardoso. Imaging and analysis of microcalcifications and lipid/necrotic core calcification in fibrous cap atheroma. *Int J Cardiovasc Imaging.* 2015;31:1079-1087.
11. Itou T, Maldonado N, Yamada I, Goettsch C, Matsumoto J, Aikawa M, Singh S, Aikawa E. Cystathionine γ-lyase accelerates osteoclast differentiation: Identification of a novel regulator

of osteoclastogenesis by proteomic analysis. *Arterioscler Thromb Vasc Biol.* 2014;34:626-634.

Supplemental Figures

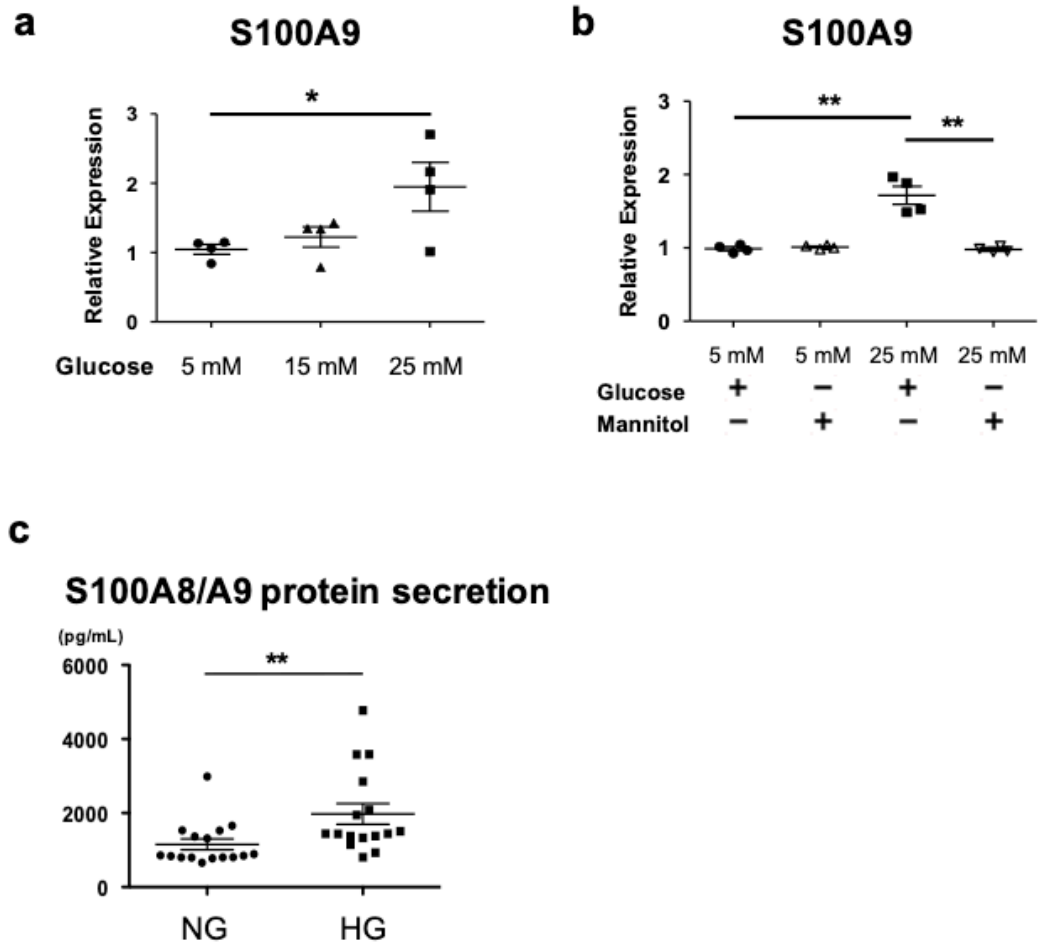

Supplementary Figure I. The effect of high glucose on S100A9 in human primary macrophages

(a) mRNA expression of S100A9 was measured in human primary macrophages after stimulation with various concentrations of glucose for 6 hours by real-time qPCR (n = 4 PBMC donors). (b) mRNA expression of S100A9 was measured in human primary macrophages after stimulation with high glucose (HG) and mannitol to maintain the same osmolarity as HG for 6 hours (n = 4 PBMC donors). (c) S100A8/A9 heterodimer levels in supernatants of human primary macrophages were measured by ELISA after administration with normal glucose (NG) and HG condition for 24 hours (n = 16 PBMC donors). P value was calculated by unpaired student's t-test or one-way ANOVA, based on a comparison with NG, followed by Bonferroni test. *P < 0.05, **P < 0.01, ***P < 0.001. Error bars indicate ± SEM.

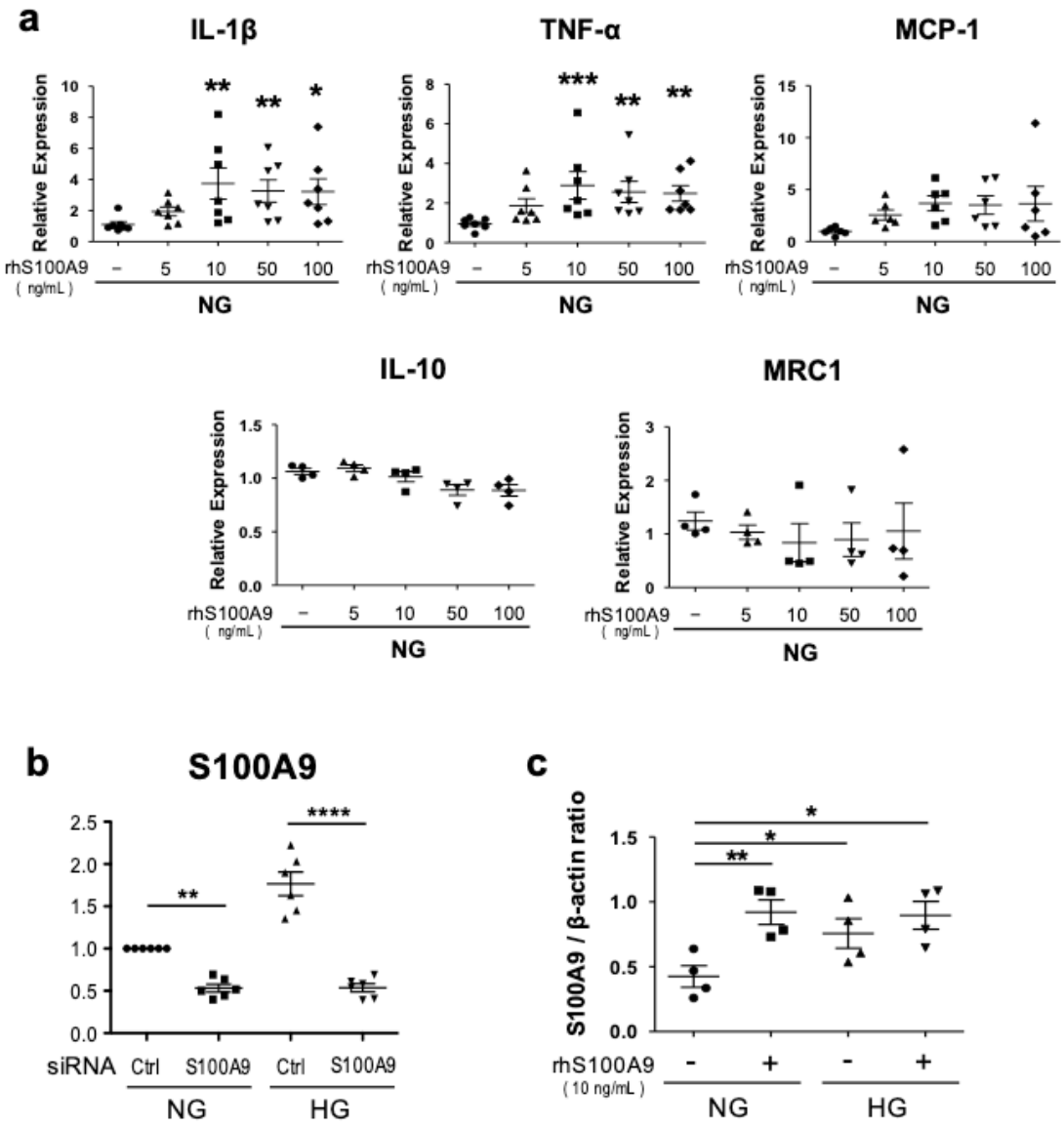

Supplementary Figure II. The effect of recombinant human S100A9 on pro-inflammatory factors in human primary macrophages

(a) mRNA expression of pro-inflammatory factors IL-1β, TNF-α and MCP-1, and anti-inflammatory factors IL-10 and MRC1, was measured in human primary macrophages after stimulation with various concentrations of recombinant human S100A9 (rhS100A9) for 6 hours (n = 4 - 7 PBMC donors). (b) The mRNA expression levels in human primary macrophages after suppression by S100A9 siRNA for 48 hours (n = 6 PBMC donors). (c) Signal intensity of S100A9 / β-actin ratio was measured within EVs derived from human primary macrophages by Western blot (n = 4 PBMC donors). P value was calculated by one-way ANOVA, based on a comparison with normal glucose (NG), followed by Bonferroni test. *P < 0.05, **P < 0.01, ***P < 0.001 , ****P < 0.0001. Error bars indicate ± SEM.

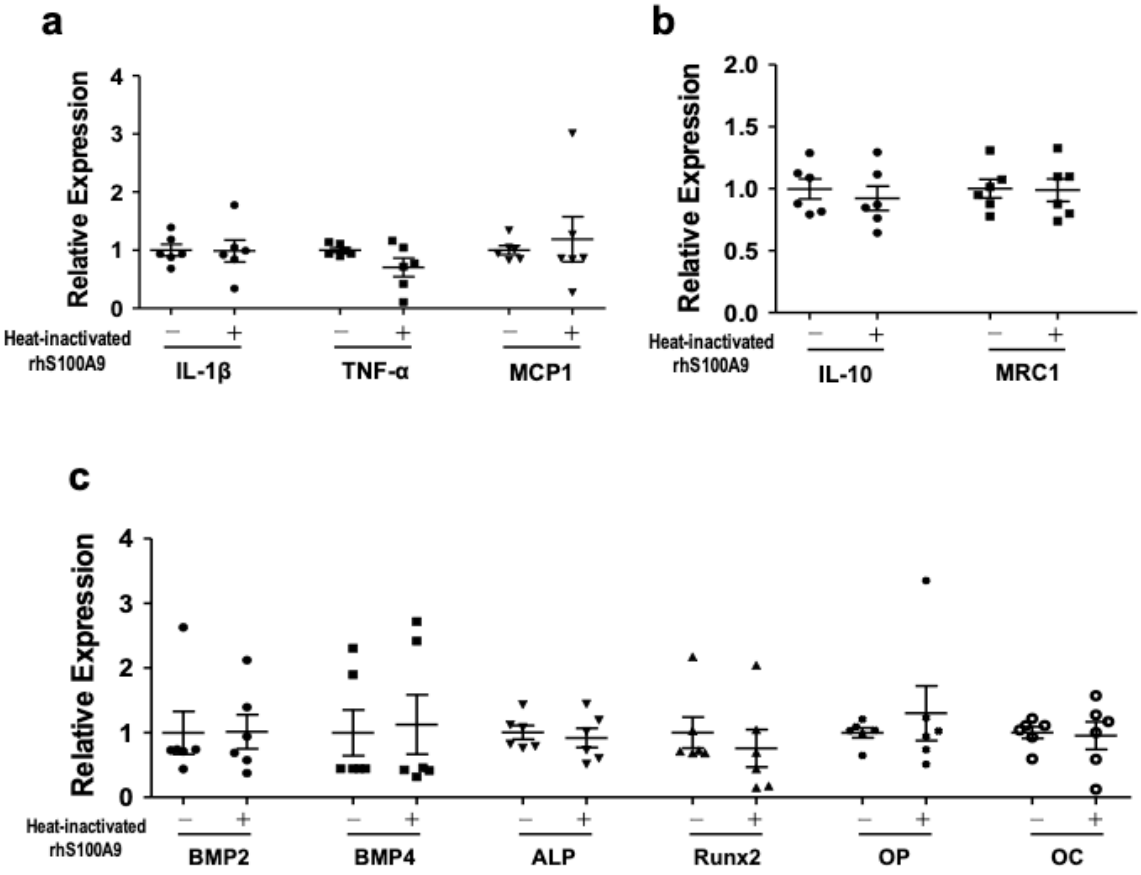

Supplementary Figure III. The effect of heat inactivated recombinant human S100A9 on pro-inflammatory, anti-inflammatory, and osteogenic factors in human primary macrophages
(a) mRNA expression of pro-inflammatory factors IL-1β, TNF-α and MCP1 was measured in human primary macrophages after exposure to normal glucose (NG) for 24 hours, followed by stimulation with heat-inactivated rhS100A9 (10ng/ml) for 6 hours (n = 6 PBMC donors). (b) mRNA expression of anti-inflammatory factors IL-10 and MRC1 was measured in human primary macrophages after exposure to NG for 24 hours, followed by stimulation with heat-inactivated rhS100A9 (10ng/ml) for 6 hours (n = 6 PBMC donors). (c) mRNA expression of osteogenic factors BMP2, BMP4, ALP, RUNX2, OP, and OC was measured in human primary macrophages after exposure to NG for 24 hours, followed by stimulation with heat-inactivated rhS100A9 (10ng/ml) for 12 hours (n = 6 PBMC donors). P value was calculated by unpaired student's t-test compared with normal glucose (NG). Error bars indicate ± SEM.

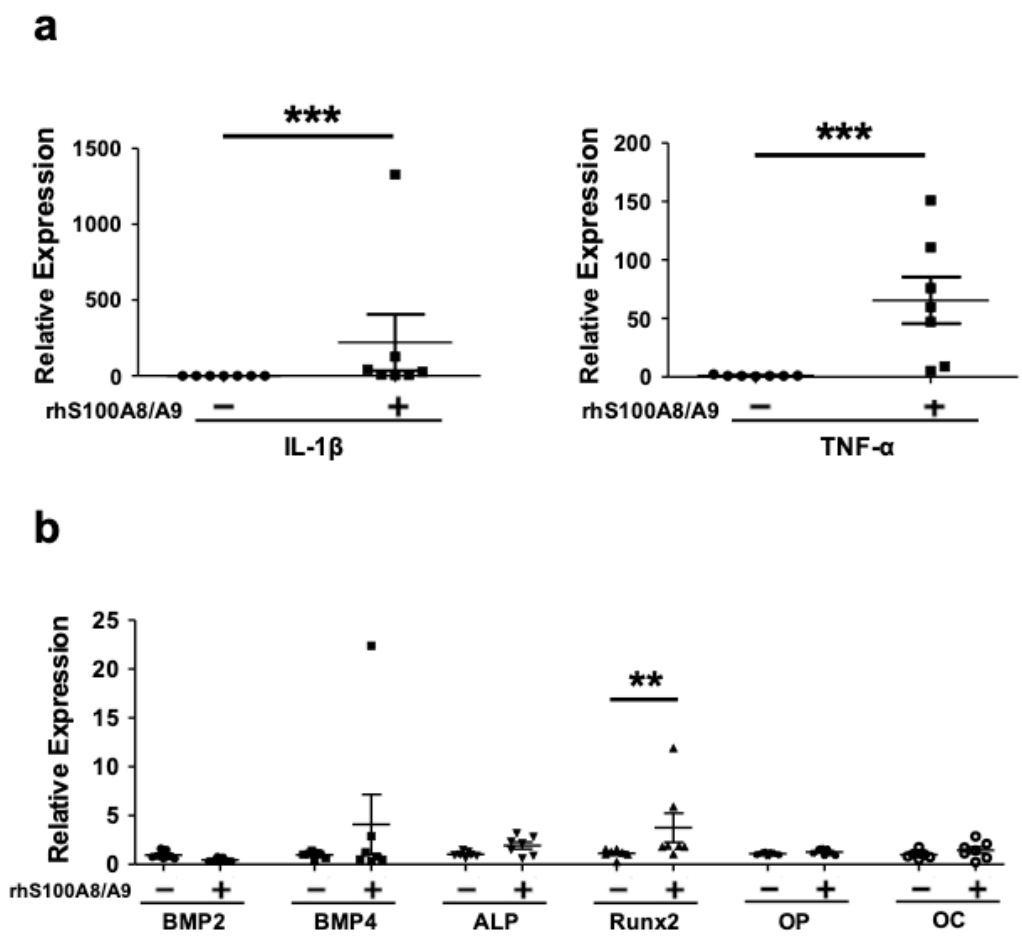

Supplementary Figure Ⅳ.The effect of rhS100A8/A9 on pro-inflammatory and osteogenic factors in human primary macrophages

(a) mRNA expression of pro-inflammatory factors IL-1β, and TNF-α was measured in human primary macrophages after stimulation with HG and rhS100A8/A9 (5 μg/ml) for 6 hours (n = 7 PBMC donors). (b) mRNA expression of the osteogenic factors BMP2, BMP4, ALP, Runx2, osteopontin, and osteocalcin was measured in human primary macrophages after stimulation with HG and rhS100A8/A9 (5 μg/ml) for 12 hours (n = 7 PBMC donors). P value was calculated by unpaired student's t-test compared with high glucose (HG). **P < 0.01, ***P < 0.001. Error bars indicate ± SEM.

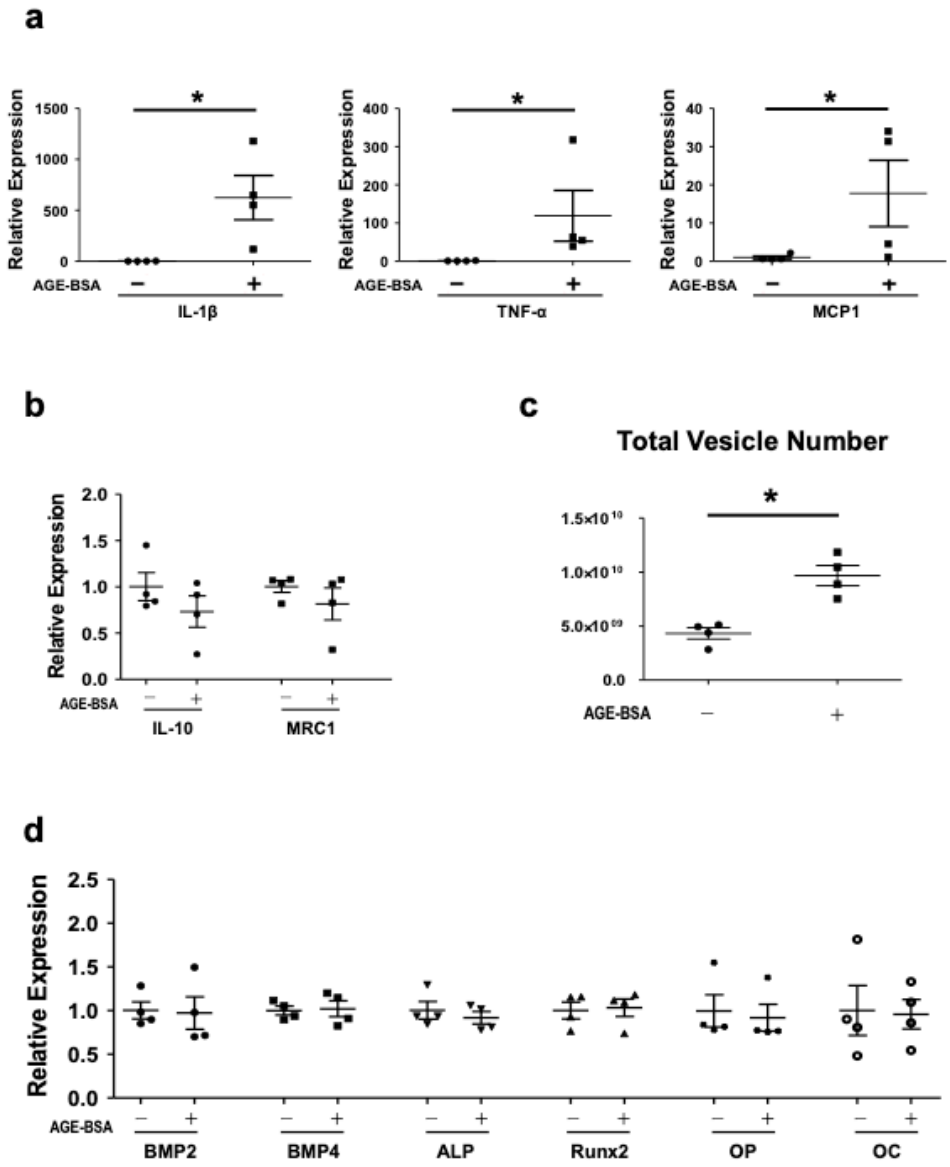

Supplementary Figure V. The effect of AGE-BSA on pro-inflammatory, anti- inflammatory and osteogenic factors, and vesicle secretion in human primary macrophages
(a) mRNA expression of pro-inflammatory factors IL-1β, TNF-α, and MCP-1 was measured in human primary macrophages after stimulation with NG and AGE-BSA (100μM) for 6 hours (n = 4 PBMC donors). (b) mRNA expression of anti-inflammatory factors IL-10 and MRC-1 was measured in human primary macrophages after stimulation with NG and AGE-BSA (100μM) for 6 hours (n = 4 PBMC donors). (c) Quantification of EVs derived from human primary macrophages after stimulation with NG and AGE-BSA (100μM) for 24 hours by nanoparticle tracking analysis (n = 4 PBMC donors). (d) mRNA expression of the osteogenic factors BMP2, BMP4, ALP, Runx2, osteopontin, and osteocalcin was measured in human primary macrophages after stimulation with NG and AGE-BSA (100μM) for 12 hours (n = 4 PBMC donors). P value was calculated by unpaired student's t-test compared with normal glucose (NG). *P < 0.05. Error bars indicate ± SEM.

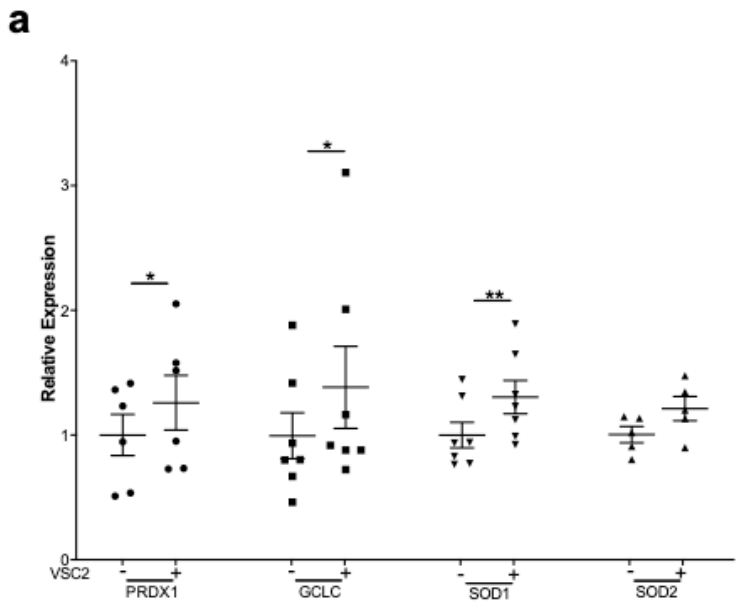

Supplementary Figure VI. Alteration in Nrf2 activity relates to changes in redox state in human primary macrophages

(a) mRNA expression of the antioxidant related genes PRDX, GCLC, SOD1, and SOD2 was measured in human primary macrophages after stimulation with HG and VSC2 (10 μM) for 1 hour (n = 5-7 PBMC donors). P value was calculated by unpaired student's t-test compared with high glucose (HG). *P < 0.05, **P < 0.01, ***P < 0.001 , ****P < 0.0001. Error bars indicate ± SEM.

a

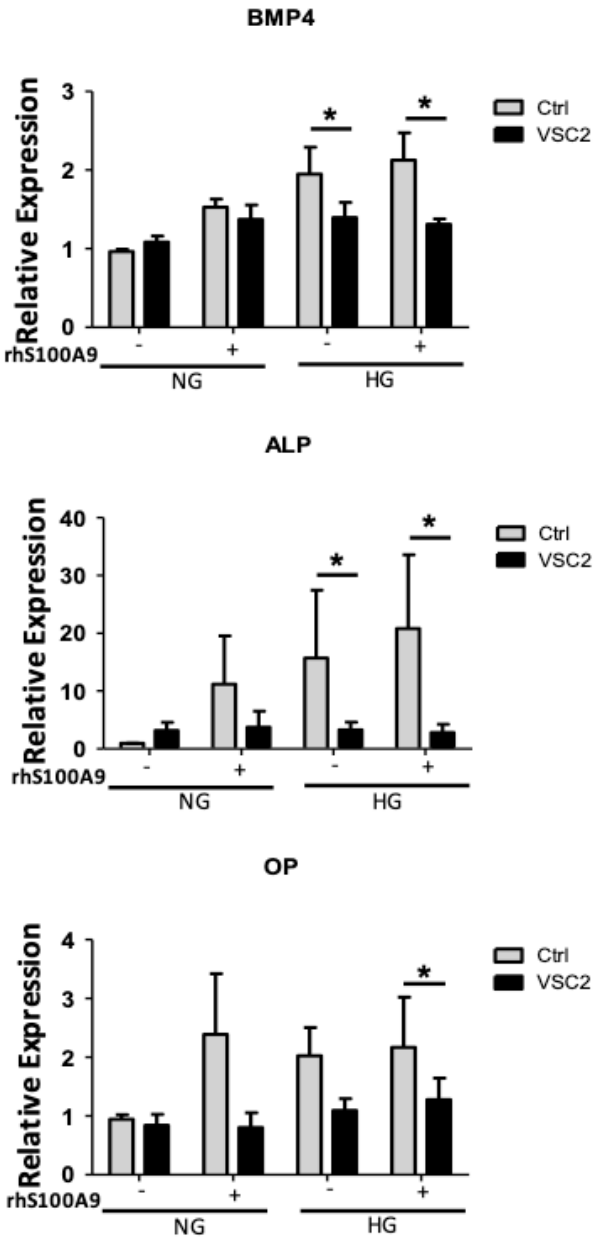

Supplementary Figure VII. Recovery of the balance between the Nrf2 and NF-κB pathways, decreases osteogenic factors within EVs derived from human primary macrophages.
(a) mRNA expression of osteogenic factors BMP4, ALP, and OP were measured in human primary macrophages after pretreatment with VSC2 (10 μM) for 1 hour and stimulation with HG and rhS100A9 for 12 hours (n = 4 PBMC donors). P value was calculated by paired student's t-test compared with high glucose (HG). P value was calculated by unpaired student's t-test compared with high glucose (HG). *P < 0.05, **P < 0.01, ***P < 0.001 , ****P < 0.0001. Error bars indicate ± SEM.

a

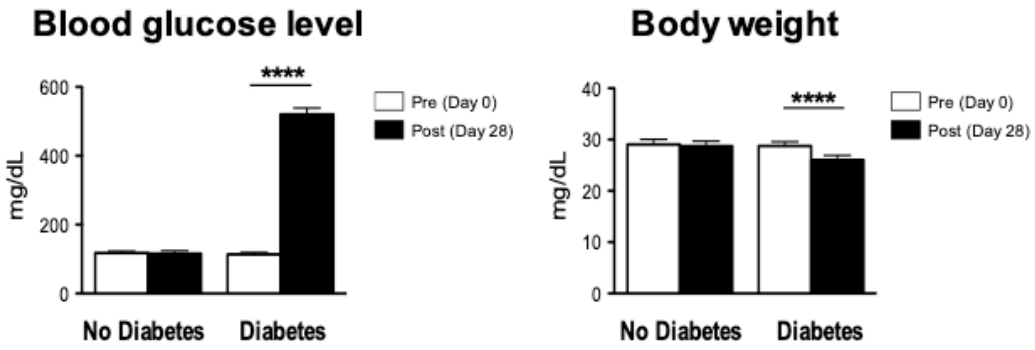

b

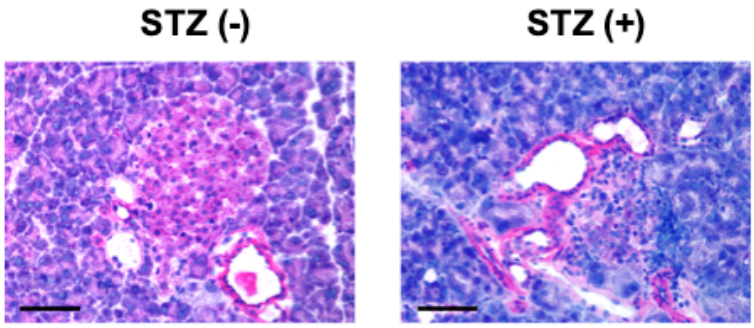

Supplementary Figure VIII . The effect of streptozocin to induce type 1 diabetes in Apoe$^{-/-}$ mice

(a) Blood glucose levels and body weight were measured in streptozocin (STZ) induced diabetic Apoe$^{-/-}$ mice before and 28 days after STZ injection (n=27-33 mice/group). (b) H&E staining of pancreas from Apoe$^{-/-}$ mice with and without STZ injection. The image represents 5 mice/group. Scale bar = 50 μm. P value was calculated by unpaired student's t-test. ****P < 0.0001. Error bars indicate ± SEM.

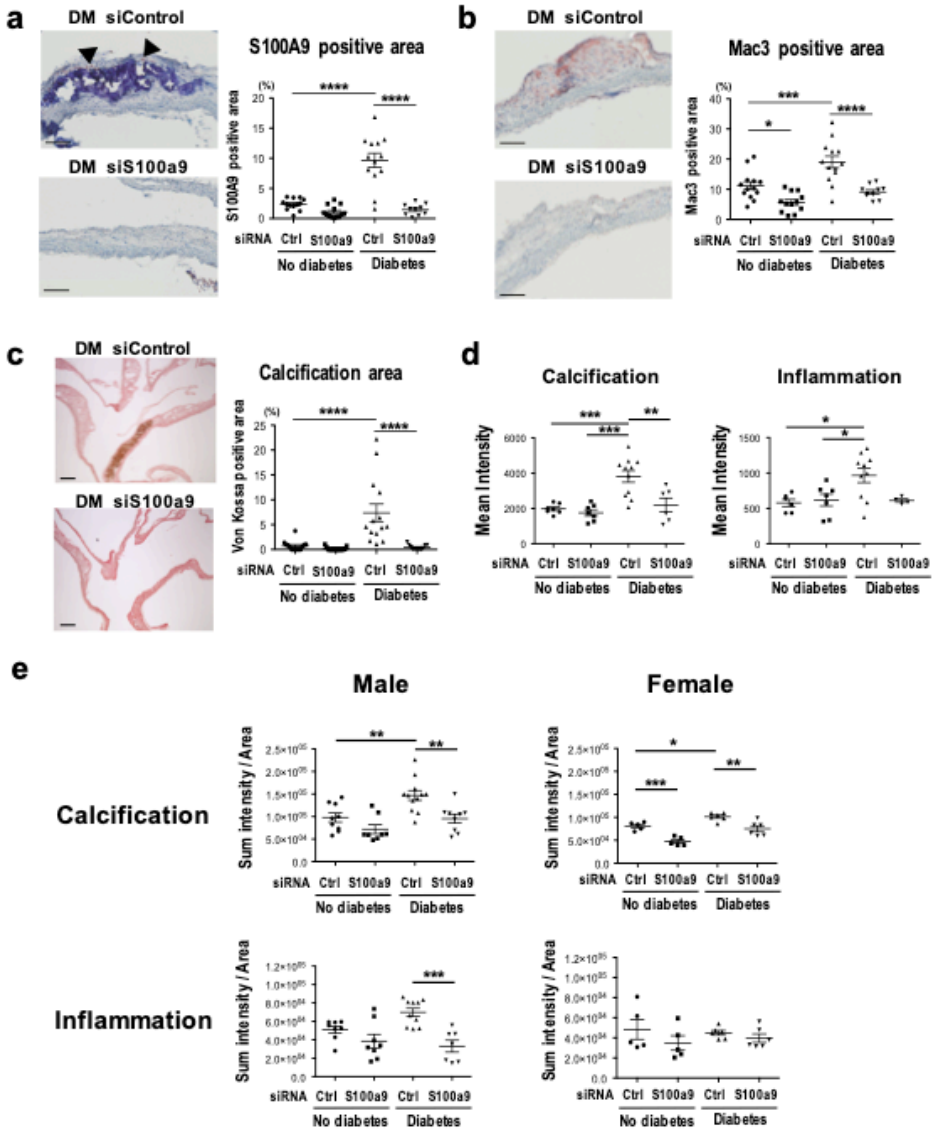

Supplementary Figure IX. The effects of Macrophage-targeted LNP containing S100A9 siRNA on atherogenesis and vascular calcification in diabetic Apoe$^{-/-}$ mice

(a) Staining for S100A9 on longitudinal sections of the aortic arch (n = 10-13). Arrowhead shows the positive area of S100A9 in plaques. Scale bar = 100 μm. The graph shows the percentage of S100A9 positive area in the plaques. (b) Mac staining on longitudinal sections of the aortic arch (n = 10-13). Scale bar = 100 μm. (c) Von Kossa staining in the aorta (n = 11-14). Scale bar = 200 μm. (d) The graph shows the mean intensity of calcification (OsteoSense 680) and Inflammation (ProSense 750) from the *in vivo* molecular imaging of carotid arteries (Figure 5D) from diabetic Apoe$^{-/-}$ mice (n = 4-11). (e) The graph shows Sum intensity related to total aortic area for FRI in male and female diabetic Apoe$^{-/-}$ mice treated with macrophage-targeted LNP containing control siRNA (siControl) or S100A9 siRNA (siS100a9). Aortic vascular calcification assessed by OsteoSense 680EX and vascular inflammation assessed by ProSense 750EX. (n = 7-12, male; n = 5-6, female). P value was calculated by two-way ANOVA followed by Bonferroni test. *P < 0.05, **P < 0.01, ***P < 0.001, ****P < 0.0001. Error bars indicate ± SEM.

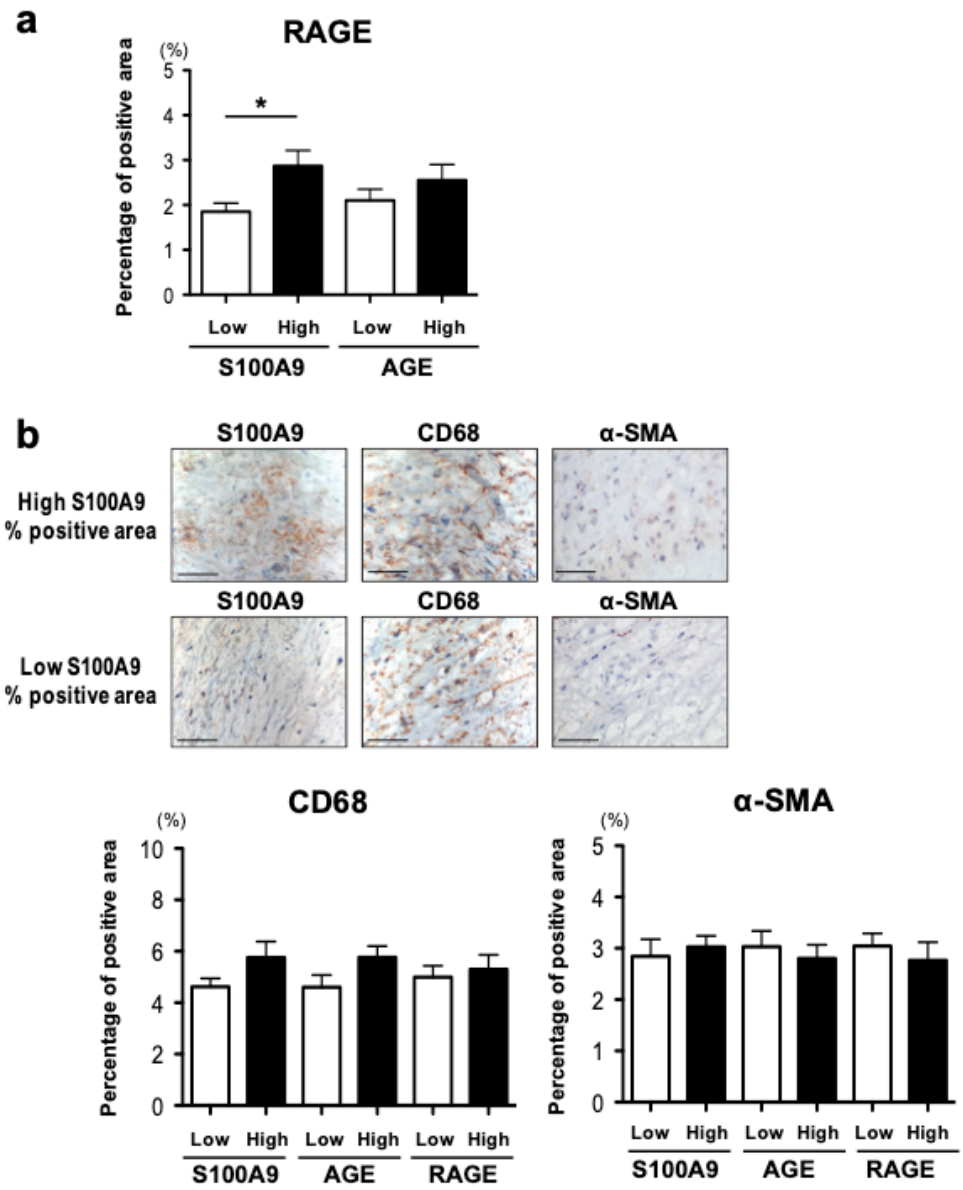

Supplementary Figure X . The effect of S100A9 in human calcified carotid arteries
25 human atheroma obtained from carotid endarterectomy. Sections were stained with anti-S100A9, -RAGE, -AGE, -CD68, and -αSMA antibodies. (a) Staining for RAGE in human atheroma. The graph shows the RAGE positive area associated with its ligands, AGE and S100A9 in serial section of human atheroma. (b) Staining for S100A9, CD68, and αSMA in human atheroma (n=25). One of high S100A9 % positive area (top panel) and low S100A9 % positive area (bottom panel) are shown. Scale bars: 50 μm. The graph shows the percentage of CD68+ and αSMA+ to S100A9+, AGE+, and RAGE+ area. The average of 5-10 high power fields was used for the analysis. P value was calculated by unpaired student's t-test. *P < 0.05. Error bars indicate ± SEM.

Supplemental Table I

Serum biochemical paramaters from diabetic and non-diabetic Apoe$^{-/-}$ mice injected with macrophage-targeted LNP containing siControl and siS100a9. There were no significant differences among these groups.

	Non-DM siControl (n=14)	Non-DM siS100a9 (n=13)	DM siControl (n=18)	DM siS100a9 (n=15)
Serum urea (mg/dL)	26.1 ± 3.4	23.6 ± 2.6	20.8 ± 1.8	23.9 ± 2.0
Serum creatinine (mg/dL)	0.18 ± 0.02	0.19 ± 0.01	0.18 ± 0.01	0.17 ± 0.02
Phosphate (mmol/L)	2.69 ± 0.03	2.74 ± 0.04	2.70 ± 0.03	2.68 ± 0.03
Calcium (mmol/L)	2.32 ± 0.03	2.34 ± 0.02	2.35 ± 0.03	2.36 ± 0.03
AST (U/L)	26.1 ± 3.7	27.5 ± 3.8	28.5 ± 3.1	31.2 ± 3.6
ALT (U/L)	22.1 ± 4.1	23.5 ± 3.8	23.3 ± 3.8	23.9 ± 4.1
Total cholesterol (mg/dL)	453.4 ± 20.3	505.0 ± 37.0	487.4 ± 22.8	460.6 ± 24.0
LDL-cholesterol (mg/dL)	311.0 ± 28.7	350.2 ± 32.1	322.4 ± 19.9	310.0 ± 28.7
HDL-cholesterol (mg/dL)	52.7 ± 6.4	49.0 ± 4.0	43.4 ± 3.0	52.0 ± 4.7

AST: Aspartate Transaminas, ALT: Alanine Transaminase

The statistical analysis was calculated by two-way ANOVA, followed by the Bonferonni test. Values indicate mean ± SEM.

Supplemental Table II

(a) Significantly enriched ($p<0.05$) proteins in diabetic patients group (DM) and non-diabetic patients group (nonDM), respectively, with a fold change cutoff of over than 2.0.

Gene_name	Fold change (DM/nonDM)	Number of unique peptides
ELANE	38.42	2
LAIR1	11.68	2
MMP7	10.41	3
AHCY	9.34	3
B4DLV7	6.88	5
B7Z507	5.43	5
PLAUR	4.79	2
PON1	4.49	14
TREM2	4.25	4
PRTN3	4.11	4
S100A8	3.90	9
GLA	3.73	2
Q59H08	3.70	6
S100A9	3.48	9
RNPEP	3.33	6
APOB	3.18	204
SLC3A2	3.16	3
GPLD1	3.07	20
APOD	3.01	11
ATP6AP1	2.96	2
CD74-ROS1_C6;R32	2.76	2
FCN3	2.71	4
ITIH2	2.64	34
Q96K68	2.62	3
Q59E93	2.44	3
SERPINE1	2.35	5
CPN1	2.31	3
HLA-A	2.24	3
ACTR3	2.22	4
OSCAR	2.18	3
C4BPA	2.09	2
A0A140VJZ4	2.04	2
LAMP1	2.03	3

(b) Significantly enriched ($p<0.05$) proteins in diabetic patients group (DM) and non-diabetic patients group (nonDM), respectively, with a fold change cutoff of less than 0.5.

Gene_name	Fold change (DM/nonDM)	Number of unique peptides
B2RBW9	0.00	2
TUBB1	0.00	6
TRIP6	0.04	4
LDB3	0.13	7
TES	0.14	11
Q53FI7	0.14	21
LMCD1	0.15	14
FHL2	0.16	22
CRIP2	0.16	10
CSRP2	0.17	10
PPP1R14A	0.17	5
CSRP1	0.22	12
A8K259	0.25	4
HPSE	0.27	2
CRIP1	0.27	4
APOC4-APOC2	0.29	7
SYNPO	0.29	6
PDLIM7	0.33	17
B7Z8X5	0.33	2
COL5A1	0.37	9
PDLIM4	0.37	8
MYH10	0.37	62
PDLIM5	0.39	4
LASP1	0.40	11
MYH11	0.40	83
TLN1	0.40	55
DAG1	0.41	4
HEL-S-34	0.41	7
B4DI63	0.41	27
APOC3	0.41	7
TAGLN2	0.42	22
CNN1	0.43	18
TBCA	0.43	2
RBP4	0.43	8
DDAH2	0.43	4
B4DUV1	0.45	7
CNN2	0.45	9
LU	0.46	9
NPTN	0.46	3
S100A13	0.47	3
COL21A1	0.48	3
HEL-S-115	0.49	12
COL1A2	0.50	11

Supplemental Table III

(a) Human primers for quantitative real time PCR

Gene	Forward primer sequence (5'-3')	Reverse primer sequence (5'-3')
Human S100A9	GTGCGAAAAGATCTGCAAAA	TCAGCTGCTTGTCTGCATTT
Human RAGE	GGCAGACAGAGCCAGGAC	AGCACCCAGGCTCCAACT
Human IL-1β	GGACAAGCTGAGGAAGATGC	TCGTTATCCCATGTGTCGAA
Human TNF-α	GACAAGCCTGTAGCCCATGT	GAGGTACAGGCCCTCTGATG
Human MCP-1	CCCCAGTCACCTGCTGTTAT	AGATCTCCTTGGCCACAATG
Human IL-10	GATGCCTTCAGCAGAGTGAA	GCAACCCAGGTAACCCTTAAA
Human MRC1	CACCATCGAGGAATTGGACT	ACAATTCGTCATTTGGCTCA
Human BMP2	CCCACTTGGAGGAGAAACAA	GCTGTTTGTGTTTGGCTTGA
Human BMP4	TAGCAAGAGTGCCGTCATTCC	GCGCTCAGGATACTCAAGACC
Human ALP	AGAACCCCAAAGGCTTCTTC	CTTGGCTTTTCCTTCATGGT
Human Runx2	CCGCCTCAGTGATTTAGGGC	GGGTCTGTAATCTGACTCTGTCC
Human Osteopontin	GAGGGCTTGGTTGTCAGC	CAATTCTCATGGTAGTGAGTTTTCC
Human Osteocalcin	TGAGAGCCCTCACACTCCTC	ACCTTTGCTGGACTCTGCAC
Human HO-1	AAGACTGCGTTCCTGCTCAA	GGGGGCAGAATCTTGCACTT
Human NQO1	TGTGATATTCCAGTTCCCCCTGC	TGGCAGCGTAAGTGTAAGCA
Human GCLC	CAGTGGTGGATGGTTGTG	ATTGATGATGGTGTCTATGC
Human PRDX1	TTGGTATCAGACCCGAAGCG	AAAGGCCCCTGAACGAGATG
Human SOD1	GCAGATGACTTGGGCAAAGG	TGGGCGATCCCAATTACACC
Human SOD2	GTCCCGGTTTTGGGGTATGTG	GCGTTGATGTGAGGTTCCAG
GAPDH	TGGGTGTGAACCATGAGAAG	GCTAAGCAGTTGGTGGTGC

(b) Mouse primers for quantitative real time PCR

Gene	Forward primer sequence (5'-3')	Reverse primer sequence (5'-3')
Mouse S100A9	CCTTCTCAGATGGAGCGCAG	TGTCCAGGTCCTCCATGATG
Mouse RAGE	CCTGGGTGCTGGTTCTTGCTCT	GATCTGGGTGCTCTTACGGTCC
Mouse IL-1β	GCCCATCCTCTGTGACTCAT	AGGCCACAGGTATTTTGTCG
Mouse TNF-α	AGCCCCCAGTCTGTATCCTT	CTCCCTTTGCAGAACTCAGG
Mouse MCP-1	AGGTCCCTGTCATGCTTCTG	TCTGGACCCATTCCTTCTTG
Mouse IL-10	CAGAGCCACATGCTCCTAGA	TGTCCAGCTGGTCCTTTGTT
Mouse MRC1	CTCTGTTCAGCTATTGGACGC	CGGAATTTCTGGGATTCAGCTTC
Mouse BMP2	GCTTCTTAGACGGACTGCGG	GCAACACTAGAAGACAGCGGGT
Mouse BMP4	AGCCCGCTTCTGCAGGA	AAAGGCTCAGAGAAGCTGCG
Mouse ALP	GGACAGGACACACACACACA	CAAACAGGAGAGCCACTTCA
Mouse Runx2	AGGGACTATGGCGTCAAACA	GGCTCACGTCGCTCATCTT
Mouse Osteopontin	CTCCATCGTCATCATCATCG	TGCACCCAGATCCTATAGCC
Mouse Osteocalcine	CCCAGACCTAGCAGACACCA	GGGACTGAGGCTCCAAGGTAG
β-actin	CCTGAGCGCAAGTACTCTGTGT	GCTGATCCACATCTGCTGGAA

Major Resources Table

Animals (in vivo studies)

Species	Vendor or Source	Background Strain	Sex	Catalog number
Apoe$^{-/-}$	The Jackson Laboratory, Bar Harbor, ME	C57BL/6J	Male and Female	Stock No: 002052
S100a9$^{-/-}$	Provided by Dr. Kevin Croce, Brigham and Women's Hospital, Harvard Medical School, Boston, MA	C57BL/6J	Male and Female	N/A

Antibodies and ELISA kits

Western blot antibody	Vendor or Source	Catalog #	Working concentration (Dilution)	Lot # (preferred but not required)
RAGE	GeneTex Inc.	GTX23611	0.33 µg/ml (1:1000)	N/A
S100A9	Abcam	Ab75478	Product Usage Information (1:1000)	N/A
Rel A (NF-kappa-B p65 subunit)	BETHYL Laboratory. Inc,	A301-824A	1.0 µg/ml (1:1000)	N/A
Phospho-NF-κB p65 (Ser536)	Cell Signaling Tecchnology	3031S	Product Usage Information (1:1000)	N/A
β-actin	Cell Signaling Tecchnology	4970S	Product Usage Information (1:5000)	N/A
Immunohistochemistry antibody	**Vendor or Source**	**Catalog #**	**Working concentration (Dilution)**	**Lot # (preferred but not required)**
AGE (human)	Bioss Antibodies	bs-1158R	10.0 µg/ml (1:100)	N/A
RAGE	Gene Tex	GTX23611	6.6 µg/ml (human; 1:50) 8.3 µg/ml (mouse; 1:40)	N/A
S100A9	Proteintech Group, Inc.	14226-1-AP	0.8 µg/ml (human; 1:250) 4.0 µg/ml (mouse; 1:50)	N/A
ALP	Abcam	ab108337	Product Usage Information (human; 1:100)	N/A
Mac3	BD Biosciences	553322	1.0 µg/ml (1:500)	N/A
CD68	Dako	M0814	Product Usage Information (1:500)	N/A
αSMA	Enzo Biochem, Inc.	ENZ-C34931	0.8 µg/ml (1:25)	N/A
Immunohistochemistry Kit	**Vendor or Source**	**Catalog #**	**Working concentration (Dilution)**	**Lot # (preferred but not required)**
Alkaline phosphatase substrate kit	Vector Laboratories	SK-5100	N/A	N/A
Immunofluorescence antibody	**Vendor or Source**	**Catalog #**	**Working concentration (Dilution)**	**Lot # (preferred but not required)**
RAGE (rabbit IgG)	Gene Tex	GTX23611	6.6 µg/ml (1:50)	N/A
ALP (rabbit IgG)	Abcam	ab108337	Product Usage Information (1:100)	N/A
S100A9 (mouse IgG)	Sino biological	11145-MM01	Product Usage Information (1:100)	N/A
Alexa Fluor anti-rabbit 568-labeled secondary antibody	Thermo Fisher Scientific	A-11011	2.0 µg/ml	N/A
Alexa Fluor anti-mouse 488-labeled secondary antibody	Thermo Fisher Scientific	A28175	1.0 µg/ml	N/A

Immunofluorescence – in situ hybridization dual staining	Vendor or Source	Catalog #	Working concentration (Dilution)	Lot # (preferred but not required)
RNAscope 2.5 HD Reagent Kit - RED	Advanced Cell Diagnostics	322350	N/A	N/A
Probe Mm-S100a9	Advanced Cell Diagnostics	481401	Product Usage Information	481401
Mac3	BD Biosciences	553322	2.5 µg/ml (1:200)	N/A
Alexa Fluor anti-rat 488-labeled secondary antibody	Thermo Fisher Scientific	A-11006	6.6 µg/m	N/A
DAPI	Thermo Fisher Scientific	D1306	300 nM	N/A
ELISA kit	**Vendor or Source**	**Catalog #**	**Working concentration (Dilution)**	**Lot # (preferred but not required)**
Urea QuantiChrom assay kit	BioAssay Systems	DIUR-100	N/A	N/A
Creatinine QuantiChrom assay kit	BioAssay Systems	DICT-500	N/A	N/A
Phosphate QuantiChrom assay kit	BioAssay Systems	DIPI-500	N/A	N/A
Calcium QuantiChrom assay kit	BioAssay Systems	DICA-500	N/A	N/A
Asparate transaminase (AST) EnzyChrom assay kit	BioAssay Systems	EASTR-100	N/A	N/A
Alanine transaminase (ALT) EnzyChrom assay kit	BioAssay Systems	EALT-100	N/A	N/A
Total cholesterol EnzyChrom assay kit	BioAssay Systems	EHDL-100	N/A	N/A
LDL/VLDL/HDL cholesterol EnzyChrom assay kit	BioAssay Systems	EHDL-100	N/A	N/A

Cultured Cells

Name	Vendor or Source	Sex (F, M, or unknown)
Buffy coat (human primary macrophage)	Research Blood Components, LLC.	unknown
THP-1 cells	ATCC	N/A

Other

Intravital microscopy and fluorescent reflection imaging	Vendor or Source	Catalog #	Working concentration (Dilution)
ProSense 750EX	PerkinElmer, Inc.	NEV10001EX	4 nmol
OsteoSense 680EX	PerkinElmer, Inc.	NEV10020EX	5 nmol